

Synthesis and Characterization of Stereospecific 1-Propargyl-2-(dimethoxymethyl)-1-cyclohexanols

Juwhan Liu¹, Sang-Il Kim¹, Seung-Yong Lee¹, Yong-Hyun Kim, Kee-Young Lee, Chang-Young Oh, and Won-Hun Ham

College of Pharmacy, SungKyunKwan University, Suwon 440-746, Korea and ¹Dept. of Polymer Science and Engineering, Chungnam National University, 220 Gung-dong, Youseong-gu, Taejon 305-764, Korea

(Received January 7, 2000)

Stereochemical isomers with hydroxy groups were synthesized by reacting 2-(dimethoxymethyl)cyclohexanone with propargylmagnesium bromide. The stereo chemical structures were identified by NMR spectral interpretation and the geometry optimization. To assist the NMR interpretation, geometry optimization based on semi-empirical AM1 and PM3 methods was applied. Throughout this study, the structures of the two isomers were all determined and ¹H and ¹³C NMR spectra were fully assigned. It was proven that the less polar isomer is an axial alcohol and the more polar one is an equatorial alcohol.

Key words: 2-(Dimethoxymethyl)cyclohexanone, Stereoisomer

INTRODUCTION

The identification and conformational characterization of stereochemical products synthesized via stereoselective routes have been of keen interest. Cyclic ketones can be converted into axial and equatorial alcohols by the reaction with organomagnesium compounds (Guillerm-Dron *et al.*, 1971). On the other hand, it is known that 2-(diethoxymethyl) ketones can be synthesized from cyclic ketones (Mock *et al.*, 1981, Suzuki *et al.*, 1982 and Herbert *et al.*, 1969). The isomer percentages of axial and equatorial alcohols depends on the reaction condition including type of substituents, solvent, and the temperature (Ashby *et al.*, 1975).

In this study, stereochemical isomers with hydroxy groups were synthesized by reacting 2-(dimethoxymethyl) cyclohexanone with propargylmagnesium bromide in diethyl ether at 0, and they were identified by NMR spectroscopic techniques. Also NMR results were interpreted for their conformational characterization with the aid of molecular modeling techniques based on AM1 (Pretsch *et al.*, 1989, Dewar *et al.*, 1985, Stewart *et al.*, 1989 and Stewart *et al.*, 1990) and PM3 (Dewar *et al.*, 1986) semiempirical methods.

Separation by column chromatography using hexane: ethyl acetate (3 : 1) resulted in a less polar compound and a more polar compound which are coded as IPA

and IPB, respectively. Initially, based on the polarity, it was suggested that IPA is an axial alcohol and IPB is an equatorial alcohol.

MATERIALS AND METHODS

2-(Dimethoxymethyl)cyclohexanone(1-A)

To 10.9 mL (0.1 mol) of Trimethyl orthoformate at -30 °C under a nitrogen atmosphere was added dropwise, with magnetic stirring over a period of 20 min, a solution of 15.0 mL (0.12 mol) of freshly distilled boron trifluoride etherate in 50 mL of methylene chloride. The mixture was then allowed to warm to 0°C, and stirring was continued for 15 min. The mixture was cooled to -78°C while a nitrogen atmosphere was maintained and 5.0 g (0.05 mol) of cyclohexanone(1-K) was added, followed by dropwise addition of 19.4 g (0.15 mol) of N,N-diisopropylethylamine over a period of 30 min, while efficient stirring was continued. After an additional 1 h (-78°C, stirring, nitrogen atmosphere), the cold reaction mixture was poured rapidly into 500 mL of saturated aqueous sodium bicarbonate solution at 25°C. More methylene chloride (200 mL) was added. After the mixture had been stirred vigorously for 10 min at room temperature. the organic phase was separated and washed with cold (0-5°C), dilute sulfuric acid, followed by extraction with cold water, The methylene chloride solution was dried over anhydrous magnesium sulfate, the solvent was removed by rotatory evaporation, and the residue was purified by column chromatography on silica gel to give 6.0 g (70%

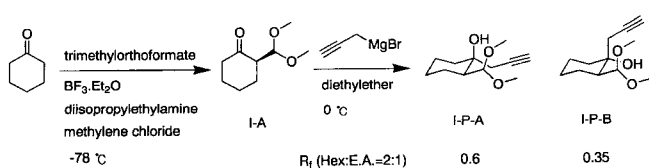
Correspondence to: Won-Hun Ham, College of pharmacy, SungKyun Kwan University, Suwon 440-746, Korea
E-mail: whham@speed.skku.ac.kr

yield) of I-A; $^1\text{H-NMR}(\text{CDCl}_3)$ d 4.69(d, 1H), 3.41(d, 6H), 2.645(m, 1H), 1.61-2.42(m, 8H).

2-(Dimethoxymethyl)-1-(2-propynyl) cyclohexanol (IPA and IPB)

To a stirred solution of 3.0 g (17.4 mmol) of 2-dimethoxymethylcyclohexanone in 50 mL diethylether at 0°C , propargyl magnesium bromide 26 mL (1.0 M) was added over 10 min. After the reaction was completed, quenched with 1 N-HCl, then organic layer was separated, washed with brine (25 mL \times 2), dried over MgSO_4 . After filtration and evaporation, the residue was purified by column chromatography on silica gel to give 2.8 g (I-P-A : I-P-B = 1.73 : 1, 76.9%) of 2-(dimethoxymethyl)-1-(2-propynyl) cyclohexanol. The reaction is shown in Scheme 1.

Several NMR experiments were performed to characterize the isomers and they include ^1H , ^{13}C , DEPT, ^1H - ^1H COSY(HH-COSY), ^{13}C - ^1H COSY(CH-COSY), and 2D NOESY. All the NMR measurements were made in CDCl_3 at 25°C on a JEOL JNM-LA300 spectrometer operating at 300.4 MHz ^1H frequency. ^1H NMR data were acquired with 45° pulse (pulse width 5.60 s), spectral width of 6,009.6 Hz, pulse delay of 4.27 s, and number of scans of 4~16. ^{13}C NMR spectra were acquired under proton decoupling with 45° pulse (pulse width 4.40 ms), spectral width of 20,366.6 Hz, pulse delay of 1.39 s, and number of scans of 64~512. DEPT ^{13}C NMR spectra were acquired with conditions similar to the proton decoupling experiments but with a longer pulse delay of 4.0 s. For all these 1D NMR techniques, 32 K of data points were used. For the HH-COSY, the spectral widths were adjusted to include only the spectral width of interest. 90° pulse was used, pulse delay was set as 0.79 s, and 512×512 data points were used. The number of scans was 16. CH-COSY experiments were performed with the same conditions as the HH-COSY except the pulse delay of 1.20 s. Also the same conditions were used for the measurements of NOESY spectra except that the pulse delay and the number of scans were adjusted as 3.0 s and 32, respectively. All the COSY and NOESY spectra were processed using the window function of sine bell or squared sine bell with the phase shift of 0° . All the data processing programs used for the display and manipulation of the spectral data are home-made and written in C++ and Fortran for a personal computer.



Scheme 1. Preparation of 2-(dimethoxymethyl)-1-(2-propynyl) cyclohexanol (IPA and IPB)

Geometry optimization of the isomers was performed using semi-empirical AM1 and PM3 methods as implemented in HyperChem 5.0 by Hypercube, Inc. The convergence was assumed to be reached when the potential energy gradients becomes 0.05 or less. Using more strict convergence criteria resulted in little progress in terms of the calculated potential energy.

RESULTS AND DISCUSSION

For the identification of isomers IPA and IPB, various 1D and 2D ^1H and ^{13}C NMR spectra were measured. For the convenience of discussion, protons and carbons will be addressed using the numbers designated in Fig. 1.

We will first try to understand most of the spectral features of ^1H NMR spectra based on plausible conformational structures and HH-COSY, CH-COSY, and NOESY NMR spectra. To gain further information on the isomers, molecular modeling techniques will be used for the conformational search. Finally, using the results thus obtained, complete assignments of ^1H , ^{13}C , and 2D NMR spectra will be attempted.

^1H NMR Spectra

1D ^1H NMR spectra of IPA and IPB are shown in Fig. 2.

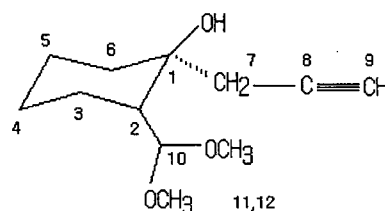


Fig. 1. Numbering scheme of protons and carbons. The hydroxy proton will be referred to simply as OH.

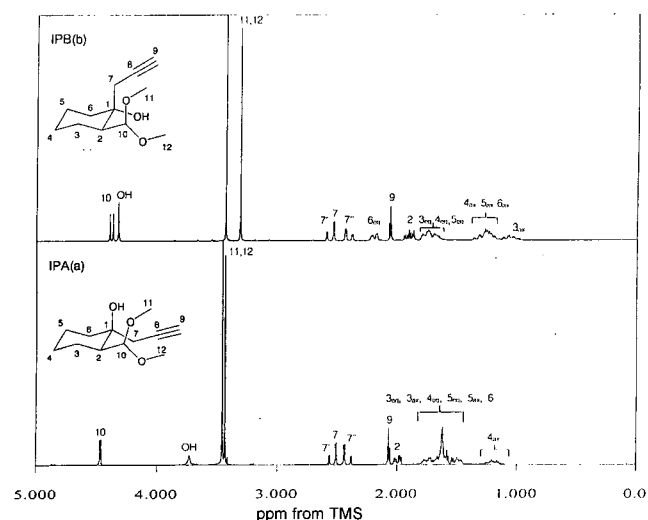


Fig. 2. 300MHz ^1H NMR spectra of isomer IPA (a) and IPB (b).

For the identification and characterization of the isomers, it was initially assumed that IPA is axial alcohol while IPB is equatorial alcohol based on their polarity as explained in the introduction section, then the NMR spectral results were interpreted accordingly. In this way, one could prove or disprove the assumption. As will be elaborated below, the assumption is considered to be proven correct.

Peaks for protons 2, 7, 9, 10, 11, 12, and OH are readily assigned based on general correlation for chemical shifts, although the exact differentiation of protons 10 and 11 is yet to be done below. Also the two 7 protons are showing AB type splitting pattern and they will be differentiated after further consideration of the spectral data and geometry optimization are made. The peaks for protons 2, 7, 10, 11, 12 and OH are showing significant differences between isomers IPA and IPB. For the proton 10 of IPA, the coupling constant is 2.9 Hz while that of IPB is 8.0 Hz. It is clear that these splittings are due to proton 2. Protons 11 and 12 appear to be experiencing more different magnetic environments in IPB than in IPA. Also, even if the overall splitting patterns are seen similar for proton 7 in IPA and IPB, the peaks 7" at higher field appear more broadened in IPB than in IPA.

The differences in the splitting patterns for proton 2 were considered along with those of proton 10. In the case of proton 2 of IPA, the splitting pattern was analysed to arise from three couplings with the strengths of 12.1 Hz, 4.0 Hz, and 2.9 Hz. In the case of IPB, the situation was similar but the related coupling constants were 12.1 Hz, 3.8 Hz, and 8.0 Hz. It is generally known that in cyclohexane and its derivatives, the coupling constants are in the range of -11~-14 Hz, 8~13 Hz, 2~6 Hz, and 2~5 Hz for geminal, axial-axial, axial-equatorial, and equatorial-equatorial couplings, respectively (Pretsch *et al.*, 1989). Here we assumed that the isomers IPA and IPB are all taking the conformation in which the dimethoxymethyl group is equatorial. This issue will be addressed again in the geometry optimization section below. Then proton 2 becomes axial, and based on the structure it can be determined that the first two values are respectively due to the coupling with 3 axial proton and 3 equatorial proton in both of IPA and IPB. Now it can be clearly seen that the last coupling constants 2.9 and 8.0 Hz for IPA and IPB, respectively, are due to proton 10. The difference in values is significant. Considering the general behavior of the vicinal coupling as a function of the dihedral angle, for example the usual Karplus curve, the coupling constant of 8.0 Hz between protons 2 and 10 is in the trans (180°) or eclipsed (0°) range while that of 2.9 Hz is in the perpendicular (90°) range. This argument is in fact true when there is no fast or significant interconversion such as ring inversion. With the bulky side groups, isomers IPA and IPB under study is believed to be stable dynamically. The latter case of 2.9 Hz corresponds to IPA and it was found that the only

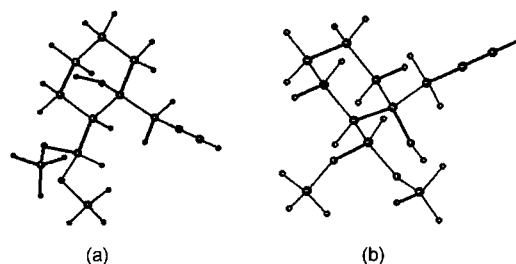


Fig. 3. Conformational structures of isomer IPA (a) and IPB (b) used in the analysis of NMR spectra, shown in stereogram. In (a) the alkylnyl group and the methoxy group at the bottom are pointing backward. On the other hand, in (b) the alkylnyl group is almost parallel to the ring plane and the methoxy group at the righthand side is pointing forward.

energetically plausible conformation satisfying the condition that the dihedral angle between protons 2 and 10 is in the vicinity of 90° is the structure shown in Fig. 3a. By the way, this structure was searched systematically using molecular modeling techniques as will be discussed below. In the case of IPB, eclipsed position between protons 2 and 10 results in severe repulsion between the dimethoxymethyl group and the other part of the molecule. Hence, similarly to IPA, a stable conformation in which protons 2 and 10 are in the trans range was searched and the result is shown in Fig. 3b. It was found that the hydrogen bonding between OH and one of the methoxy groups plays a significant role in both of the conformational structures for IPA and IPB.

IPA. Each pair of the ring protons 3 to 6 assume equatorial and axial positions and the corresponding proton peaks are normally show up at different chemical shifts. CH-COSY spectra reveal the peak positions of the

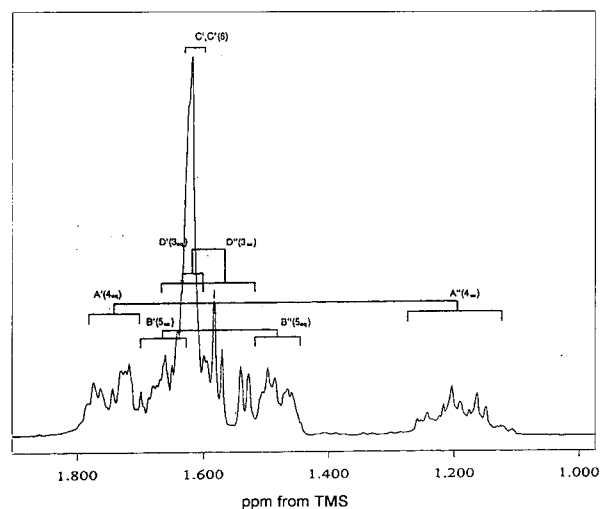


Fig. 4. Part of the ^1H NMR spectrum of IPA. Geminal protons are shown connected and the results of assignment are given in parentheses.

equatorial and axial protons attached to a carbon. Using that information, all the pairs of geminal protons were detected and the result is shown in Fig. 4. Each peak corresponding to a proton was designated as A', A'', etc., and the axial and equatorial protons will be expressed as 3_{ax} , 3_{eq} , etc.

To assign the peaks, HH-COSY and NOESY spectra were measured and are respectively shown in Fig. 5 and Fig. 6.

Peak 2 is shown to be correlated with a group of peaks around 1.52~1.64 ppm. Considering the chemical structure, they are readily recognized as peak 3 (D' and D'' in Fig. 3). Further assignment based only these 2D spectra was not straightforward than initially expected due to severe

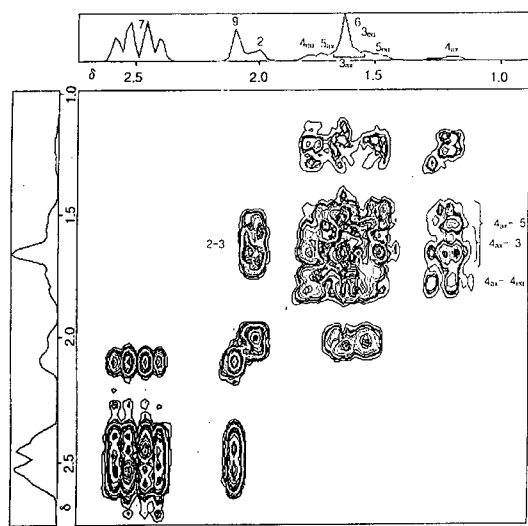


Fig. 5. HH-COSY spectrum of IPA along with the projections.

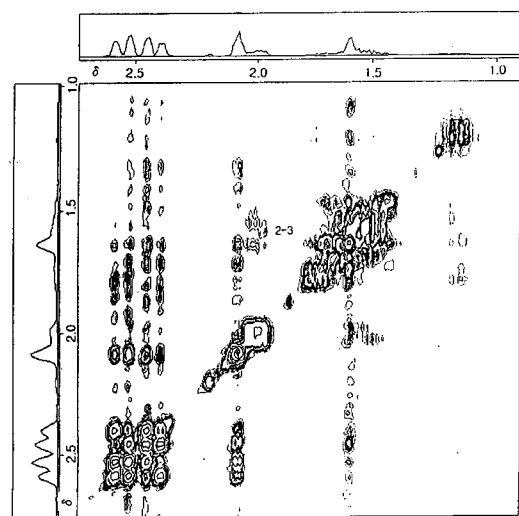


Fig. 6. NOESY spectrum of IPA along with the projections. The spectrum was not symmetrized to take noise into consideration.

overlap of peaks. So we noted that the peak group A'' corresponds to a single proton and the splitting pattern is a typical one resulting from three strong couplings on the order of 12 Hz and two weak couplings on the order of 4 Hz (i.e., each peak in 1 : 3 : 3 : 1 large splitting is split again to small 1 : 2 : 1 pattern). Considering the magnitudes of coupling constants found in cyclohexanes, only 4_{ax} or 5_{ax} proton can give such a pattern. Among the two, 5_{ax} can be excluded because 5_{ax} will be significantly deshielded by the equatorial OH group. In ref. 6, the corresponding substituent effect is reported as large as +0.46 ppm. Then A'' is 4_{ax} and A' is 4_{eq} . Now in Fig. 5, HH-COSY spectrum of IPA indicates that 4_{ax} proton is showing several couplings. Proton 3 (equatorial and axial) is already assigned. So excluding the contributions from 4_{ax} - 4_{eq} and 4_{ax} -3, there still remain some crosspeaks which must be due to 4_{ax} -5 couplings. In this way, regions B' and B'' in Fig. 4 can be assigned to 5 protons. The remaining peak groups C' and C'' are naturally assigned to the last proton 6.

For further differentiation between axial and equatorial protons in B (proton 5) and D (proton 3), it was required to consider the detailed splitting patterns. In the case of B, the region B'' shows two groups of peaks separated by 11.4 Hz. Since 5_{eq} has just one strong coupling with 5_{ax} and four weak couplings with 4_{ax} , 4_{eq} , 6_{ax} , and 6_{eq} while 5_{ax} has three strong couplings with 5_{eq} , 3_{ax} , and 4_{ax} and two weak couplings with 4_{eq} and 6_{eq} , it can be concluded that B'' corresponds to 5_{eq} while B' to 5_{ax} . In the case of D, D'' covers more wider range than D'. The righthand side of D'' shows well-separated two groups of peaks separated by 12.0 Hz each one consisting of two peaks separated by 3.6 Hz. To see if the same pattern emerges, we simulated a partial NMR spectrum using DSYMPC (Haegeler *et al.*, 1993). Only the full pattern for 3_{eq} and 3_{ax} was of interest so that only those protons that can be coupled significantly with 3_{eq} and 3_{ax} protons were considered and they are 2, 4_{eq} , and 4_{ax} . Although it is possible that 5_{eq} gives coupling of around 1 Hz via the effective planar zig-zag (or W-shape) configuration, that effect is ignored in the simulation. For the peak positions of 2, 3_{ax} , 3_{eq} , 4_{ax} , and 4_{eq} , we used 1.99 ppm, 1.59 ppm, 1.63 ppm, 1.18 ppm, and 1.75 ppm, respectively, all converted into Hz assuming 300 MHz NMR. All the geminal coupling constants were set to -12 Hz. All the vicinal axial-axial couplings were set to 10 Hz, while all the other types of vicinal couplings were set to 4 Hz. These chemical shifts and coupling constants were broadly estimated from the ^1H NMR spectrum. The result of simulation after applying line broadening with a factor of 1.5 Hz is shown in Fig. 7.

The area of 3_{eq} and 3_{ax} are overlapped with C', C'' (proton 6), and B' (Proton 5_{ax}) in the experimental spectrum but the aforementioned pattern of the righthand side of D'' is clearly seen to be reproduced. As a result,

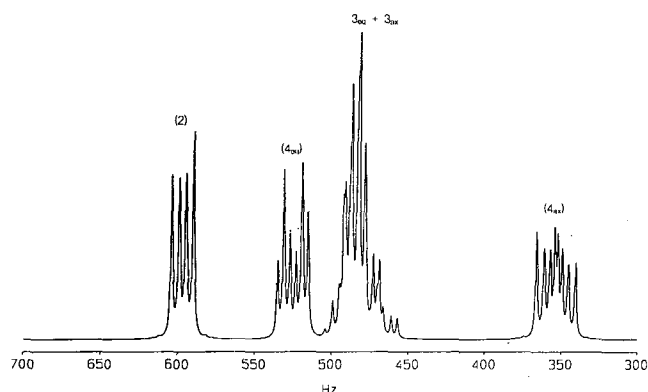


Fig. 7. Results of simulation for a partial spin system of IPA centered on 3_{eq} and 3_{ax} . Only the couplings to 3_{eq} and 3_{ax} are fully considered.

D'' was able to be assigned as 3_{ax} and D' as 3_{eq} . As a summary, the assignment results are given in the previous Fig. 4.

So far, all the assignments are made except the differentiation of 11 and 12. At this point, one may recall that the general correlation on the 1H chemical shifts tells that a proton in the region around a C-C single bond experiences shielding. This results in about 0.5 ppm upfield shift (i.e. -0.5 ppm shift) of the axial peaks compared with equatorial peaks in conformationally frozen cyclohexanes. However, in the current case, several protons are showing contrary trends. First, 5_{ax} resonates at around 1.70 ppm while 5_{eq} resonates at 1.48 ppm. For 3_{eq} and 3_{ax} , the chemical shifts were estimated to be about 1.63 and 1.59 ppm, respectively. Also both 6_{eq} and 6_{ax} are seen to appear at around 1.62 ppm. In the case of 3_{ax} and 5_{ax} , they are close to the axial OH group and experience significant downfield shifts as mentioned before. As for the 6_{ax} , it is believed that the alkynyl group is located adjacent to 6_{ax} to cause deshielding of the latter.

IPB. A procedure similar to that of IPA was applied to the spectral interpretation of the ring protons of IPB. The result is shown in Fig. 8.

Since OH and dimethoxymethyl groups are axial and the propargyl group is pointing outward of the ring, all the equatorial protons are resonating at lower field than all the corresponding axial protons as usual. It is seen that the 6_{eq} proton is resonating at much lower field than other equatorial protons. This may be explained from the conformational geometry shown in Fig. 3b. The 6_{eq} proton is located close to the alkynyl group. Moreover the location is the deshielding region due to the latter. In the same structure, one of the 7 protons ($7''$) that is pointing outwardly of the ring forms a zig-zag conformation with 6_{ax} proton for an efficient coupling of about 1.2 Hz. This coupling results in a more broadened $7''$ peaks compared

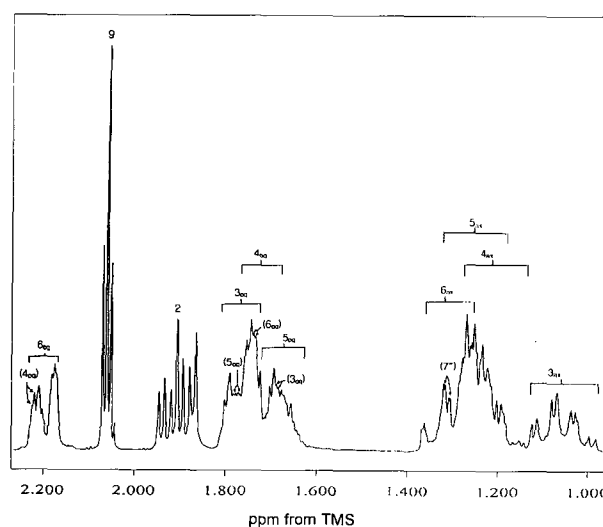


Fig. 8. Part of the 1H NMR spectrum of IPB with the assignments. The peak splittings pointed by double arrows are due to the couplings with the protons specified in parenthesis.

with $7''$ peaks and minute splittings in 6_{ax} peaks.

At this point, it seems the right place to describe the molecular modeling works to obtain detailed information on conformational structures of the isomers before further analysis is made.

Conformational analysis

IPA. The dihedral angle is defined as 0° for cis position and increases when the front group in Newman projection is rotated anticlockwise relative to the rear group. In order to find stable conformations, two dihedral angles ϕ_1 and ϕ_2 were considered in which ϕ_1 is the entral angle of $HO-C_1-C_7-C_8$ and ϕ_2 is that of $H_2-C_2-C_{10}-H_{10}$. Three angles trans (t: 180°), gauche⁺ (g^+ : 60°), and gauche⁻ (g^- : -60°) were consecutively assigned to ϕ_1 and ϕ_2 , respectively, then geometry optimization was performed for each of the nine initial conformations using the semi-empirical AM1 and PM3 methods. The result is collected in Table I.

In the table, t, g^+ , and g^- should be taken as the initial angles but not the optimized angles. However, in most

Table I. Potential energies of IPA optimized by AM1 and PM3 from the initial conformations defined by two dihedral angles ϕ_1 and ϕ_2 . PM3 energies are given in parenthesis. Energies are reported relative to the energy of (g^+ , t) which is -3387.90 Kcal/mol for AM1 and -3372.35 Kcal/mol for PM3

	ϕ_1	ϕ_2		
		t	g^+	g^-
	t	-1.31(1.54)	0.0(ref.)	3.18(4.35)
	g^+	2.02(3.68)	2.23(2.62)	1.29(1.90)
	g^-	-1.50(1.49)	1.20(1.54)	1.28(1.89)

cases, the dihedral angles j_1 and j_2 of an optimized structure were similar to those of its initial structure. To obtain each of the optimized potential energies in Table I, the conformations of methoxy groups was also considered and the lowest energy was reported. In the case of the hydroxy group, the orientation of the O-H bond was found to be automatically settled to one that can form hydrogen bonding whenever the possibility arises. It was found that the conformation of the methoxy groups plays a significant role in determining the optimized energy values.

The optimized energies show notable differences between AM1 and PM3. In the case of IPA, NMR spectral data, especially the H_2 - H_{10} coupling, suggest no considerable contribution from the conformations with $\varphi_2 = t$. The energies calculated by AM1 tells that the (t, t) and (g^- , t) conformations are the most significant ones, which is contrary to what NMR data suggests. On the other hand, PM3 results tells that, as expected, the (t, g^+) conformation is the dominant one and the other conformations are unstable by 1.49 Kcal/mol or more.

The ability of AM1 and PM3 to model intermolecular and intramolecular hydrogen bonding has been discussed in the literature (Jurema *et al.*, 1993). It was suggested that, for intermolecular hydrogen bonding, AM1 often incorrectly favors bifurcated structures with symmetrical charge distributions. Though we are not at the position to seriously judge the ability of AM1 to model the isomers under study and the solvent effect was not considered, PM3 seems correctly predicting the energies.

The most stable PM3 result is already shown above in Fig. 3a. In this conformation, $\varphi_1 = -175^\circ$ and $\varphi_2 = 78^\circ$. The distance between the OH proton and the oxygen atom of the methoxy group involved in hydrogen bonding was 2.78Å.

In the course of the geometry optimization with the dimethoxymethyl group at the equatorial position, it was noticed that there exist another series of conformations that are stabilized by the hydrogen bonding. They involve axial dimethoxymethyl group and equatorial hydroxy group, hence will be called 'inverted' conformations hereafter. Stable conformations in the inverted state were searched by varying the angles φ_1 and φ_2 as above. Interestingly enough, all the three conformations corresponding to $\varphi_2 = t$ showed potential energies lower than (in terms of AM1) or comparable to (in terms of PM3) the regular (t, g^+) conformation. The optimized energies were as follows (AM1 values are given first followed by PM3 values in parentheses): (t, t) = -0.03 (3.92), (g^+ , t) = -1.80 (0.75), (g^- , t) = 0.65 (1.83). The especially large discrepancy of (t, t) values was double checked. The lowest energy conformation of the inverted state (g^+ , t) is shown in Fig. 9.

In the inverted structures, the distance between protons 10 and 4_{ax} was 2.47Å and that between protons 10 and 6_{ax} was even closer 1.89Å. Hence if the inverted

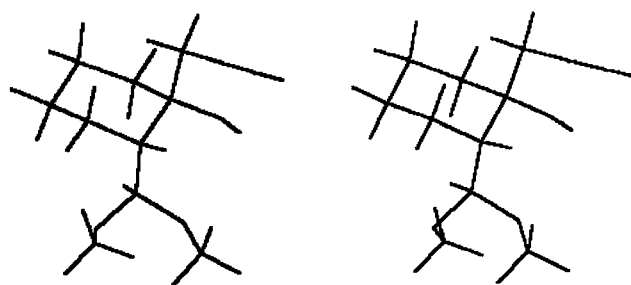


Fig. 9. The lowest energy conformation of the inverted state of IPA in stereogram

conformations do exist at room temperature, these pairs will give strong NOE crosspeaks in NOESY spectra. However, no such evidence was found. Again, it seems PM3 is superior in modeling the isomers under study. But, to be careful, we wish to mention the possibility that, while some of the regular and inverted structures may be comparably stable, at the time of synthesis, only the equatorial dimethoxymethyl versions could be created due to the fact that the starting compound 2-(dimethoxy methyl)cyclohexanone will assume almost exclusively equatorial conformation in terms of the dimethoxymethyl group position.

IPB. Similar procedures were applied to IPB as in IPA. The result is summarized in Table II.

The lowest energy conformation (g^+ , t) is already shown in Fig. 3b. This and two other lower energy conformations (t, t) and (g^- , t) all involve $\varphi_2 = t$ and are forming intramolecular hydrogen bonding. In the case of PM3, the (g^+ , g^+) conformation has a lower energy of 0.93 Kcal/mol, and this conformation can be obtained by simply rotating the dimethoxymethyl group of (g^+ , t) about 60° clockwise with respect to the ring. Both of the AM1 and PM3 results show that the (g^- , t) conformation has a lower energy. In that conformation, the optimized φ_2 was -39° and that of (g^+ , t) was 69° . However, the persistence the coupling between $7''$ proton and 6_{ax} proton with a strength of 1.2 Hz suggests that the orientation of the propargyl group is rather fixed at the lower energy conformation.

Unlike the case of IPA, the inverted conformations of IPB were found to have energies of about 5 Kcal/mol

Table II. Potential energies of IPB optimized by AM1 and PM3 from the initial conformations defined by two dihedral angles φ_1 and φ_2 . PM3 energies are given in parentheses. Energies are reported relative to the energy of (g^+ , t) which is -3389.73 Kcal/mol for AM1 and -3372.25 Kcal/mol for PM3

		φ_2		
		t	g^+	g^-
φ_1	t	0.49(1.75)	7.47(5.09)	5.43(5.12)
	g^+	0.0(ref.) (0.0)(ref.)	2.02(0.93)	3.22(2.54)
	g^-	0.68(0.25)	5.64(1.94)	2.85(3.12)

or higher relative to the references.⁷ It is because, in the inverted state, the geometry does not allow for hydrogen bonding to be formed to stabilize the conformation while steric hindrances among the ring and the substituent groups are severe.

Combining the results of the geometry optimization and NMR spectra data discussed above, the dominant conformation of IPA is (*t*, *g*⁺) in which the equatorial dimethoxymethyl group is rotated so that intramolecular hydrogen bonding can be formed (Fig. 3a). Intramolecular hydrogen bonding is also playing a significant role in IPB so that the dominant conformation is (*g*⁺, *t*) (Fig. 3b). With these results at hand, we now return to the problem of NMR spectral assignments.

It is rather straightforward to evaluate the dipole moment once a semi-empirical quantum mechanical calculation is performed. Using PM3, we calculated the dipole moments of IPA and IPB. They were 1.56 and 1.71 for IPA and IPB, respectively. This result is well consistent with the experimental observation that IPA is less polar than IPB.

Further analysis of NOESY spectra The optimized structures of IPA and IPB are shown schematically in Fig. 10. NOESY spectra of IPA and IPB are respectively

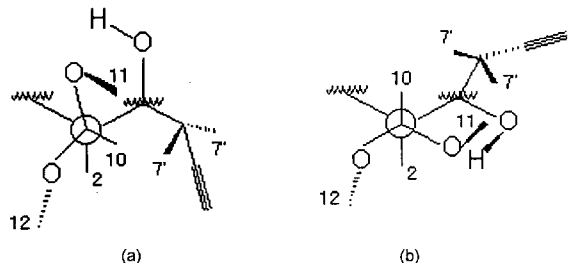


Fig. 10. Structures of IPA (a) and IPB (b) optimized by PM3

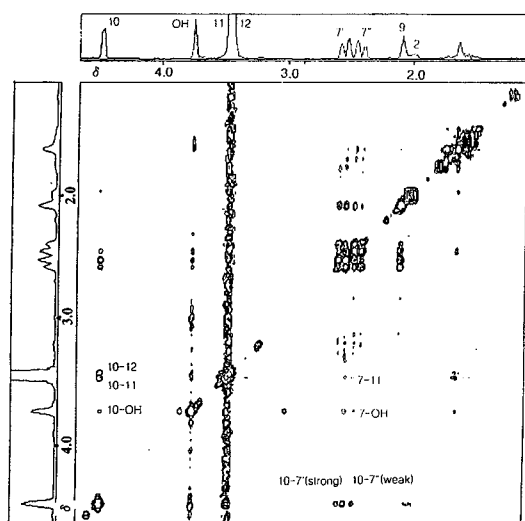


Fig. 11. NOESY spectrum of IPA along with projections

shown in Fig. 11 and Fig. 13.

These NOESY spectra suffer from noises including *t*₁-noise, so symmetrization was not applied for the interpretation not to be misled by noise. So we concentrated on such crosspeaks that their presence and intensity levels can clearly be distinguished from noise. The NOE crosspeaks of 10-12 and 10-11 in the NOESY spectrum of IPA shown in Fig. 11 have equal intensities. But 10-7' crosspeak clearly appears stronger than 10-7". Also only 7-11 is shown while 7-12 is missing. These features fit well with the structure given in Fig. 10a. The methoxy and hydroxy region is expanded and is shown in Fig. 12. It seems there exists stronger correlation between OH and proton 11 than between OH and 12. Again this phenomenon is consistent with the proposed structure.

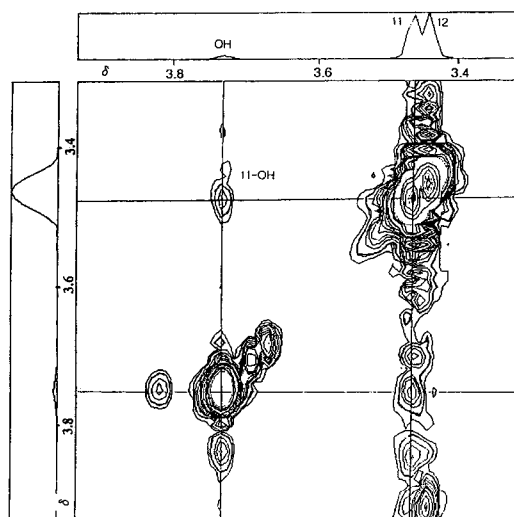


Fig. 12. OH and methoxy region of the NOESY spectrum of IPA along with projections

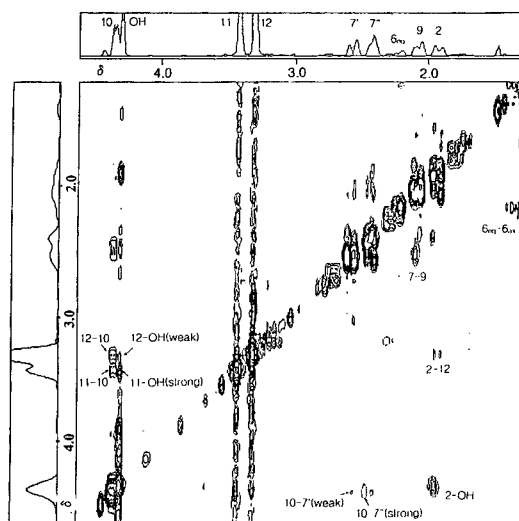


Fig. 13. NOESY spectrum of IPB along with projections

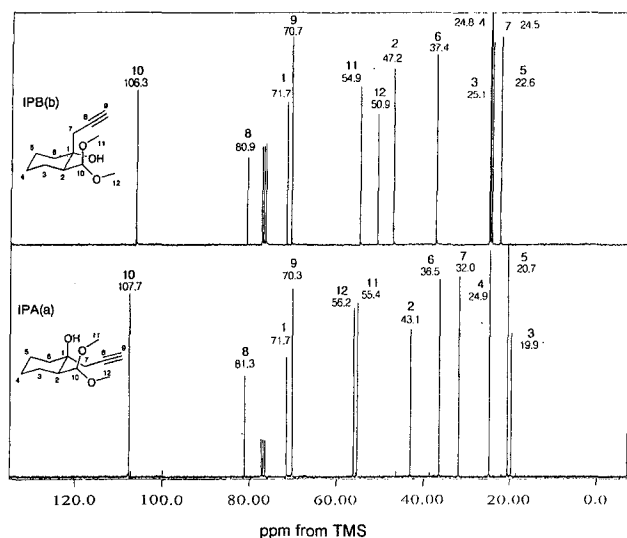


Fig. 14. 75 MHz ^{13}C NMR spectra of isomers iPA (a) and IPB (b).

In the case of IPB shown in Fig. 13, 10-7'' and 11-OH appear stronger than 10-7' and 12-OH, respectively. Also, while 2-12 is present, 2-11 is not. So one can know that 7'' is closer to 10 than 7'. As for the methoxy protons 11 and 12, 12 is closer to 2, while 11 is closer to OH. Since protons 11 are closer to both the dimethoxymethyl and hydroxy groups than protons 12, it is expected the former is more deshielded than the latter.

^{13}C NMR Spectra It is a relatively simple problem to assign ^{13}C NMR spectra once the ^1H NMR spectra are fully assigned and CH-COSY spectra are given. The ^{13}C NMR spectra are shown in Fig. 14 with the assignments.

These assignments were confirmed with ^{13}C DEPT spectra. Although, due to the lack of detailed substituent effect data, we didn't analyse the data further, a detailed analysis of the substituent effects of ^{13}C chemical shifts in terms of the stereochemical structures will lead to corroborate the ^1H NMR spectral interpretation.

CONCLUSION

NMR spectral interpretation and the geometry optimization were consistent in elucidating the stereochemical structures of 1-propargyl-2-(dimethoxymethyl)-1-cyclohexanol isomers synthesized by reacting 2-(dimethoxymethyl)cyclohexanone with propargylmagnesium bromide. The conformations of both of the isomers were proven to be stable without undergoing ring inversions based on the magnitude of the coupling constants between axial and equatorial protons and the interproton distances. Also it was shown that the intramolecular hydrogen bonding is playing a significant role in determining the confor-

mations. To assist the NMR interpretation, geometry optimization based on semi-empirical AM1 and PM3 methods was applied. It was suggested that AM1 is not adequate in estimating the conformational structures of the isomers under study. Throughout this study, the structures of the two isomers were all determined and ^1H and ^{13}C NMR spectra were fully assigned. It was proven that the less polar isomer is an axial alcohol and the more polar one is an equatorial alcohol.

ACKNOWLEDGEMENTS

The financial support from the Korea Science and Engineering Foundation (KOSEF 98-0403-12-01-3) is greatly acknowledged.

REFERENCES

- Ashby, E. C., Laemmle, J. T. Stereochemistry of organo-metallic compound addition to ketones. *Chemical Review*, 75, 521-546 (1975).
- Dewar, M. J. S., Zoebisch, E. G., Healy, E. F., Stewart, J. J. P., A new general purpose quantum mechanical molecular model. *J. Am. Chem. Soc.*, 107, 3902-3909 (1985).
- Dewar, M. J. S., Dieter, K. M., Evaluation of AM1 calculated proton affinities and deprotonation enthalpies. *J. Am. Chem. Soc.*, 108, 8075-8086 (1986).
- Guillerm-Dron, D., Capmau, M. L., Chodkiewicz, W. C. *R. Acad. Sci., Ser. C*, 273, 759 (1971).
- Haegle, G., Spiske, R., Hoeffken, H. W., Lenzen, T., Weber, U., Goudetsidis, S., *Phosphorus, Sulfur and Silicon*, 77, 262 (1993).
- Herbert, O. H., Leonard, J. C., Martin, G., Hugh, D. O., The chemistry of carbanions. XVIII. Preparation of trimethylsilyl enol ethers. *J. Org. Chem.*, 34, 2324-2336 (1969).
- Jurema, M. W., Shields, G. C., Ability of the PM3 quantum mechanical method to model intermolecular hydrogen bonding between neutral molecules. *J. Comput. Chem.*, 14, 89-104 (1993).
- Mock, W. L., Tsou, H-R., A procedure for diethoxy-methylation of ketones. *J. Org. Chem.*, 46, 2557-2561 (1981).
- Pretsch, E.; Siebl, J.; Sumon, W.; Biemann, K., *Table of Spectral Data for Structure; Determination of Organic Compounds*, 2nd ed., (1989).
- Stewart, J. J. P., Optimization of parameters for Semi-empirical methods II. Applications. *J. Comput. Chem.*, 10, 221-264 (1989).
- Stewart, J. J. P., MOPAC: A Semi-empirical molecular orbital program. *J. Comput. Aided Mol. Design*, 4, 1-105 (1990).
- Suzuki, M., Yanaisawa, A., Noyori, R., Regiospecific aldalkoxymethylation of preformed enolates. *Tetrahedron Lett.*, 23, 3595-3396 (1982).